NANO LETTERS

pubs.acs.org/NanoLett Letter

Near-Unity Light Absorption in a Monolayer WS_2 Van der Waals Heterostructure Cavity

Itai Epstein,*,▽ Bernat Terrés,▽ André J. Chaves, Varun-Varma Pusapati, Daniel A. Rhodes, Bettina Frank, Valentin Zimmermann, Ying Qin, Kenji Watanabe, Takashi Taniguchi, Harald Giessen, Sefaattin Tongay, James C. Hone, Nuno M. R. Peres, and Frank H. L. Koppens*

Cite This: *Nano Lett.* 2020, 20, 3545−3552 Read Online

ACCESS | Metrics & More | Article Recommendations | Supporting Information

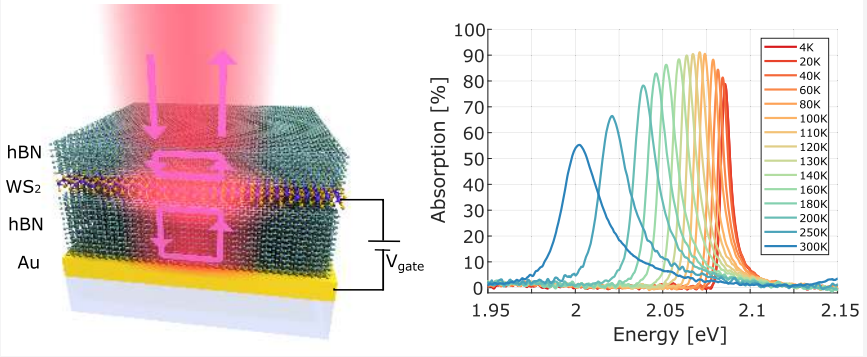

ABSTRACT: Excitons in monolayer transition-metal-dichalcogenides (TMDs) dominate their optical response and exhibit strong light−matter interactions with lifetime-limited emission. While various approaches have been applied to enhance light-exciton interactions in TMDs, the achieved strength have been far below unity, and a complete picture of its underlying physical mechanisms and fundamental limits has not been provided. Here, we introduce a TMD-based van der Waals heterostructure cavity that provides near-unity excitonic absorption, and emission of excitonic complexes that are observed at ultralow excitation powers. Our results are in full agreement with a quantum theoretical framework introduced to describe the light−exciton−cavity interaction. We find that the subtle interplay between the radiative, nonradiative and dephasing decay rates plays a crucial role, and unveil a universal absorption law for excitons in 2D systems. This enhanced light−exciton interaction provides a platform for studying excitonic phase-transitions and quantum nonlinearities and enables new possibilities for 2D semiconductor-based optoelectronic devices.

KEYWORDS: *TMD Excitons, Unity absorption, 2D materials, Light-matter interaction, Exciton complexes*

The remarkable properties of excitons in monolayer TMDs, together with the ability to readily control their charge carrier density, have attracted a significant amount of interest in recent years. This has led to the observation of numerous phenomena,[1,2] such as higher-order exciton complexes,[3−6] coupled spin-valley physics,[1,7−10] single photon quantum emitters,[11−15] together with monolayer semiconductor-based lasers, light-emitting-diodes, and photodetectors.[16−20] Excitons in monolayer TMDs exhibit strong interaction with light, both in absorption and photoemission processes,[2,21−23] which facilitates large photovoltaic response enabled by strong peaks in the joint density of states[24] and strong-coupling,[25,26] to name two examples. Unlike their counterparts in quantum-well semiconductors, excitons in TMDs practically dominate the optical response of the material.[2,22] This stems from their large binding energies, which are a result of the strong Coulomb interaction and reduced screening that arise from their low dimensionality.[27] The existence of robust excitonic states deep within the bandgap results in an optical bandgap that differs significantly from the electronic one[28] and, thus, prevails over the standard electronic-based optical response.

Nevertheless, in absolute values, the absorption of light by excitons in monolayer TMDs is far below unity, ranging between 2−12% for as-transferred monolayers,[5,29−32] and about 20−30% with the aid of a cavity.[33−35] Similarly, 5−7% absorption have been previously reported for trions.[36,37] Using thicker TMDs, higher and broadband absorption has been observed, but the thickness was over 20 monolayers.[38] More

Received: February 5, 2020
Revised: April 6, 2020
Published: April 13, 2020

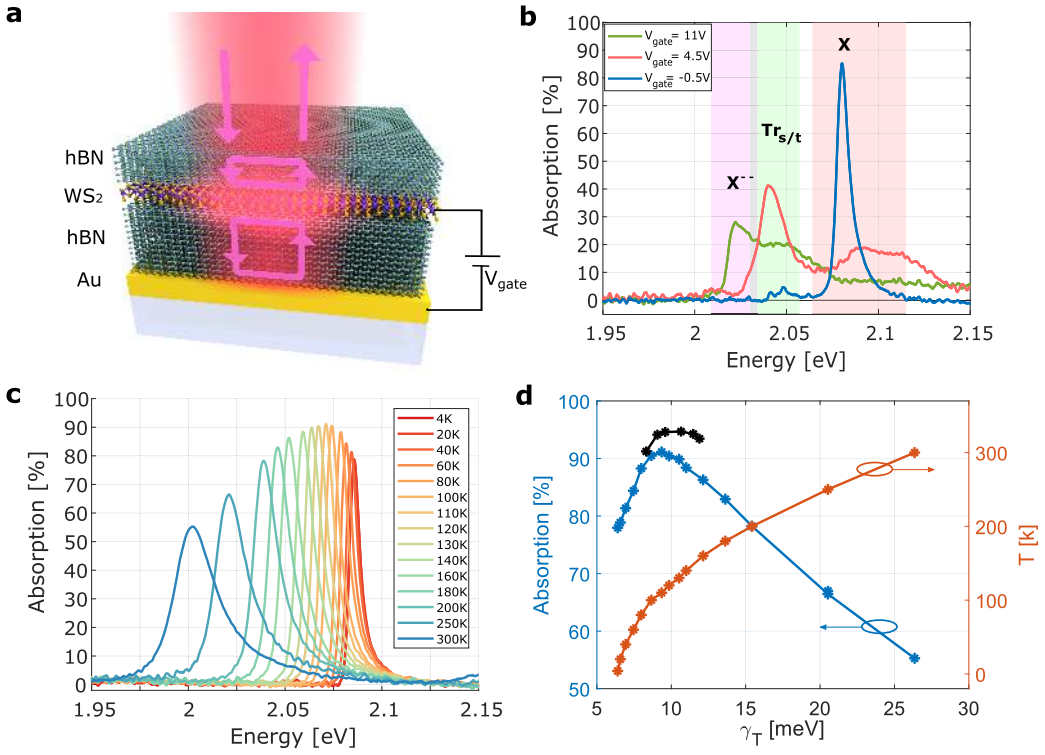

Figure 1. Light−exciton interaction in a van der Waals heterostructure cavity. (a) The structure of the VHC: a 15 nm hBN/monolayer WS_2/30 nm hBN heterostructure with optimized hBN thicknesses is transferred on top of a gold back-reflector. The gate voltage V_{gate} controls the doping in the WS_2. (b) Gate-dependent spectral absorption for sample U2, showing ∼85% excitonic absorption, ∼41% trion absorption, and ∼28% of the next negatively charged trion state, at voltages $V_{gate} = -0.5$ V, $V_{gate} = 4.5$ V, and $V_{gate} = 11$ V, respectively. (c) Temperature-dependent excitonic spectral absorption from sample U1, showing the nontrivial behavior of the absorption, and a maximum absorption of ∼92% at $T = 110$ K. (d) Maximum excitonic absorption dependency on the total line width γ_T for sample U1 (blue curve) and the temperature-dependent exciton line width (red curve). The black curve shows the measured absorption from sample U3, reaching a maximal value of 95%.

complex cavities have also been proposed,[39−41] but have not been realized to date. Thus, the question remains whether the achievable interaction strength can be pushed further and what would its limit be? Can unitary absorption be experimentally reached by excitons in an atomic thin layer? The answers may play an important role in the understanding of excitonic complexes in TMDs, and the realization of practical 2D material optoelectronic devices.

Here, we demonstrate ultrastrong light-exciton interaction in a WS_2-based high quality van der Waals heterostructure cavity (VHC), that is, an optical cavity built from van der Waals (VdW) materials, which can be controlled both electrically and optically. While the cavity is quite broadband, the near-unity absorption is attainable owing to four major elements: (1) achievable narrow excitonic line widths, owing to the VdW heterostructure,[42,43] (2) the ability to carefully balance the interplay between the radiative and nonradiative decay rates, γ_r and γ_{nr}, respectively, (3) the enhancement of the vacuum radiative decay rate, $\gamma_{r,0}$, via the Purcell factor, shifting the maximum absorption to larger (and more attainable) line widths, and (4) obtaining extremely low dephasing rate, $\gamma_d \ll \gamma_r, \gamma_{nr}$.

We show that this approach yields a large photoexcited excitonic population, with record values of ∼95% excitonic absorption, ∼41% for singlet and triplet trion states, and even the observation of the next negatively charged trion state with ∼28% absorption. In addition, it enables the observation of biexcitons photoluminescence (PL) at ultralow continuous-wave (cw) laser powers down to a few nW, which is 3 orders of magnitude lower than previously reported values.[44,45] We introduce an analytical approach to describe the light−exciton−cavity interaction, which is based on the semiconductor Bloch equations combined with a quantum transfer matrix method. The model takes into account the contribution of both the exciton radiative and nonradiative decay rates, γ_r and γ_{nr}, which have already been shown to affect the high reflection of monolayer TMDs.[46−48] In addition, we include the existence of a pure dephasing rate, γ_d, to account for loss of coherence during the multiple interferences within the cavity.[46] We find that the relation between γ_r and γ_{nr} establishes the condition for maximal absorption, and its limit is set by the value of the pure dephasing rate γ_d, basically limiting the coherence of the system. Experimentally, we control the nonradiative channels with temperature and the radiative channels via the geometrical parameters of the VHC (Purcell effect). Finally, we demonstrate the existence of a universal absorption law for excitons in 2D systems in this class of devices.

The VHC is composed of a monolayer WS_2 encapsulated by hexagonal-boron-nitride (hBN), with top and bottom thicknesses of 15 and 30 nm, respectively, and transferred on top of a gold back-reflector (Figure 1a). From the optical point of view, this structure forms an asymmetric Fabry−Perot cavity. The simplest case of such a cavity with a thin absorbing layer on top of a dielectric layer and a mirror is known as the Salisbury screen. In this configuration, the thickness of the dielectric is set to a quarter wavelength of the light to achieve constructive interference at the position of the absorbing layer.

https://dx.doi.org/10.1021/acs.nanolett.0c00492
Nano Lett. 2020, 20, 3545−3552

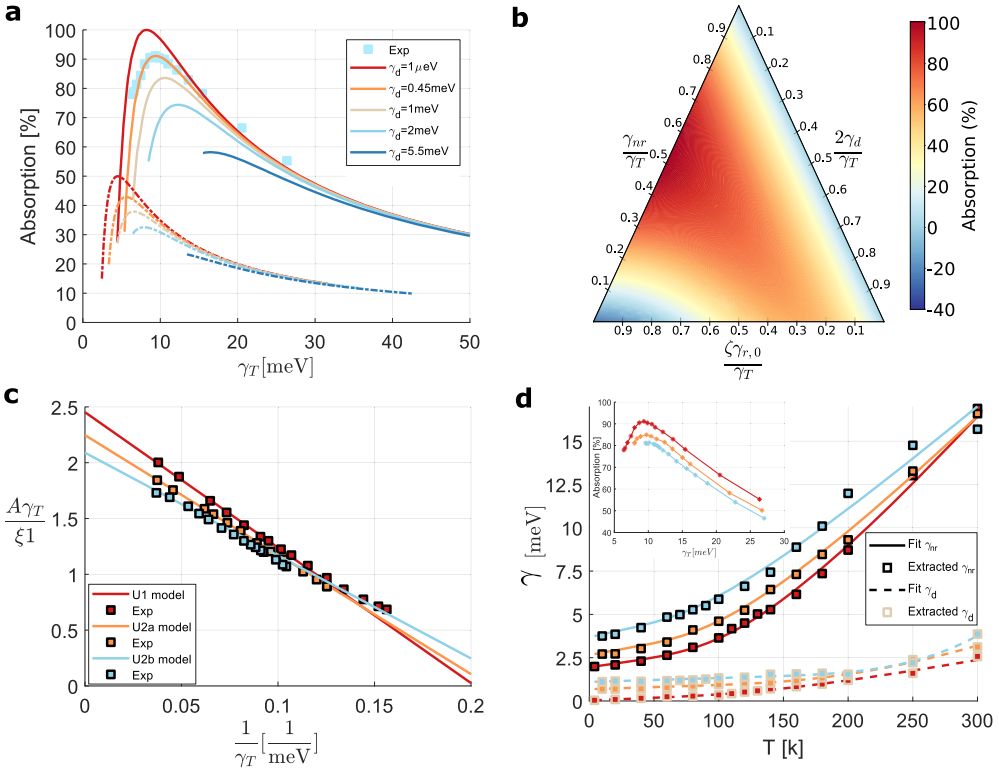

Figure 2. Analytical modeling of the light−exciton−cavity interaction. (a) Calculated absorption dependence on γ_T, for the VHC (solid lines) and a suspended TMD (dashed lines), for several dephasing values. The squares show the experimental results from sample U1. (b) Calculated maximal absorption as a function of the three normalized radiative decay rates. 100% absorption is achieved when $\gamma_d = 0$ and $\zeta\gamma_{r,0} \approx \gamma_{nr}$. The negative absorption observed at the bottom left corner is due to the dominance of γ_r and is associated with high reflection. (c) Temperature-dependent experimental results for the two different samples, U1 and U2, fitted with eq 3 exhibiting the universal absorption law. The different radiative decay rates can also be seen at the crossing of the lines with the *y*-axis. U2a and U2b correspond to two different locations on sample U2 that were chosen due to different values of the total line width at 4 K. (d) Extracted γ_{nr} and γ_d and their phenomenological fit, showing the correlation between the achievable absorption (inset) and the decay rates.

However, these are not sufficient conditions to achieve strong or near-unity abortion, as the amount of absorption is always limited by the physical properties of the thin layer. For example, placing a TMD on top of such a quarter wavelength cavity was predicted to achieve a maximum of ∼33% absorption.[34] However, building a TMD-incorporated cavity with a van der Waals heterostructure, as we implemented with the VHC, enables in situ tuning and balancing of the nonradiative and radiative rates of high-quality excitons, which is the key factor in controlling the highest possible absorption. Combining this with careful design of the cavity and integrating it with the 2D-material heterostructure leads to an attainable near-unity absorption of an atomically thin monolayer. Specifically for the VHC, the additional top hBN layer, which is required for the encapsulation, together with the penetration depth into the gold mirror, require an optimization of the final structure (see Supporting Information, SI).

Owing to the well-known inhomogeneity of TMDs,[47] we have fabricated several VHC samples: in sample U1, we used for the back-reflector a single crystalline, atomically flat gold flake,[49] while in samples U2 and U3, we used a standard evaporated gold film as the back reflector, which in sample U2 has also been used for electrostatic gating. In these structures, the optical transmission (for visible light) is zero, and the absorption can be obtained from $1 - \frac{R}{R_0}$, where R and R_0 are the reflection from the structure with and without the TMD, respectively.

A typical absorption spectra obtained from sample U2 for different gate voltages at T = 4 K is presented in Figure 1b. An absorption value as high as ∼85% can be seen at an energy of E = 2.08 eV, corresponding to the WS_2 neutral exciton (X), an absorption value of ∼41% at E = 2.041 eV, corresponding to both singlet and triplet trions (Tr_t/Tr_s) (see SI), and an absorption value of ∼28% at E = 2.023 eV, corresponding to the next charged state of the trio should be marked with two superscript minuses, X^{--} (see SI). All energetic positions of the absorption peaks and separations are in agreement with previous reports on WS_2.[6,50,51] By changing the gate voltage we control the charge carriers in the WS_2, and thus the relative spectral weights of (X), (Tr_t/Tr_s) and (X^{--}),[36,51] that is, the absorption spectrum can be controlled electrically. To the best of our knowledge, these are record absorption values together with the first observation of the (X^{--}) peak in an absorption spectra of TMDs. These are a direct result of the strong light-matter interaction provided by the VHC.

To study the ultimate absorption limits, we vary the temperature, which controls the excitonic line width, as presented in Figure 1c and d. While the exciton line width shows a continuous decrease with decreasing temperature (Figure 1d red curve), as known for the ground state exciton in semiconductors[52] and TMDs,[42,53] the excitonic absorption shows a nonmonotonic temperature dependence. An absorption value of 55% can already be seen at room-temperature, which increases to a maximum value of ∼92% at T = 110 K, and then decreases rapidly to ∼77% at T = 4 K (Figure 1d,

https://dx.doi.org/10.1021/acs.nanolett.0c00492
Nano Lett. 2020, 20, 3545−3552

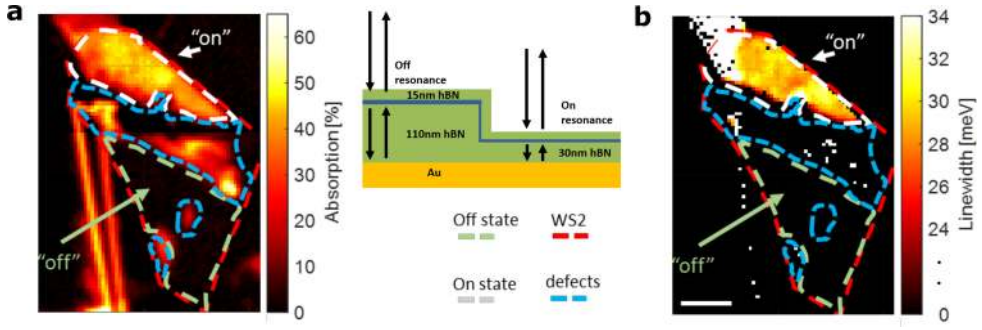

Figure 3. Tuning the excitonic optical response via the geometrical design of the VHC. (a) Spatial distribution of the absorption at room temperature showing the "on"-state for the area of maximal interaction and "off"-state at the area of minimal interaction. The schematic shows the structure of the sample with two different bottom hBN thicknesses. (b) Spatial distribution of the measured line width of the excitonic absorption in panel (a) showing a clear correlation between line width and absorption. The scale bar represents 5 μm.

blue curve), the low-temperature limit of our cryostat. Under similar conditions we obtained a maximal absorption value of ~95% for sample U3, as presented in Figure 1d (black curve) (see also SI).

To understand the physical origin of this behavior, we developed a theoretical formalism that combines an equation of motion method for the exciton, which is similar to the well-known (interacting) Bloch equations,[54,55] together with a quantum transfer matrix method (QTMM, see SI). To take into account the pure dephasing, the QTMM treats the electromagnetic fields as operators, rather than classical fields. This provides the relation between the polarization operator and the field in the 2D material. The solution, which describes the optical response of the TMD, leads to the an Elliott-type formula appropriate for the 2D material.[55] This allows us to calculate the absorption, via the reflection operator's expectation value, taking into account the contributions of both $\gamma_{r,0}$ (and its Purcell enhancement), γ_{nr}, and γ_d. The latter is important to consider, not only since the absorption is affected by pure dephasing[46] but also since a simple classical Gaussian broadening model cannot describe well the experimental behavior (see SI).

Following this approach (see SI), the maximum absorption can then be approximated by

$$A_{max} = \xi_1 \frac{\gamma_{r,0}}{\gamma_T}\left[1 - \xi_2\left(1 + 2\frac{\gamma_d}{\gamma_T}\right)\frac{\gamma_{r,0}}{\gamma_T}\right] \quad (1)$$

with

$$\gamma_T = \gamma_{nr} + 2\gamma_d + \zeta\gamma_{r,0} \quad (2)$$

where $\frac{\gamma_T}{\gamma_{r,0}}$ and $\frac{\gamma_d}{\gamma_T}$ are the normalized vacuum radiative decay and dephasing rates, and the coefficients ξ_1, ξ_2, and ζ are (see SI) parameters depending on the geometry, defined by the sizes and dielectric functions composing the different parts of the cavity, with ζ representing the Purcell factor, and $\gamma_r = \zeta\gamma_{r,0}$ being the renormalized radiative decay rate. As the trion contribution to the susceptibility is not Lorentzian owing to the self-energy term that includes exciton−electron interaction, which stems from the two-particle Green's function,[56,57] the same approach cannot be applied for the analysis of the trion response.

To expose the roles of the different decay rates in the absorption behavior, we show in Figure 2a the calculated absorption dependence on the exciton line width, γ_T, for several dephasing values. For each γ_d, $\gamma_{r,0}$ is kept constant, as it does not depend on temperature, and we vary γ_{nr} (solid lines). For the simple case of negligible γ_d, we obtain a matching condition for the maximum absorption point: $\gamma_{nr} \approx \zeta\gamma_{r,0}$ (see SI), and 100% absorption. This implies that the relation between γ_r, and γ_{nr}, rather than their absolute values, sets the matching condition for maximal absorption, and γ_d sets the limit of the absolute achievable absorption when the matching condition is fulfilled. For comparison, the absorption of a suspended monolayer is presented for the same dephasing values (dashed curves), exhibiting the same behavior and showing the known maximal absorption limit of 50% for a thin layer,[58] but at smaller and less attainable γ_T. Thus, the VHC not only enables near-unity absorption, but via the Purcell effect, also shifts the matching condition to larger γ_T, making the experimental realization of such large absorption easier to implement.

For the more general case, including finite dephasing, the matching condition translates to a more complex relation between $\frac{\gamma_{r,0}}{\gamma_T}$ and $\frac{\gamma_d}{\gamma_T}$. A ternary plot of the absorption as a function of the normalized radiative, nonradiative and pure dephasing decay rates, is presented in Figure 2b, showing all the possibilities in the decay rates' space. It can be seen from Figure 2a that away from the matching condition, the dephasing has little effect and the absorption decreases following two different regimes. For very small γ_T, $\gamma_{r,0}$ dominates the line width and the absorption decreases as the TMD becomes highly reflective (corresponding to negative absorption, as seen in (Figure 2b).[46−48] For very large γ_T, γ_{nr} and γ_d dominates the line width and the absorption is decreased as the TMD becomes transparent. The value of γ_d varies from sample to sample and is likely due to the variations in the quality of the obtained sample, and more specifically on their disorder and doping levels, which are the results of the material quality itself and on the fabrication quality.

The above-discussed decay rates are highly dependent on the cavity design, TMD quality, fabrication-induced interface quality, and can vary locally.[47] Yet, via a simple representation of eq 1 as a function of γ_T^{-1}, the model makes a striking prediction and inescapable universal feature of this class of devices:

$$\frac{A_{max}\gamma_T}{\xi_1} = \gamma_{r,0}\left[1 - \xi_2\left(1 + 2\frac{\gamma_d}{\gamma_T}\right)\frac{\gamma_{r,0}}{\gamma_T}\right] \quad (3)$$

https://dx.doi.org/10.1021/acs.nanolett.0c00492
Nano Lett. 2020, 20, 3545−3552

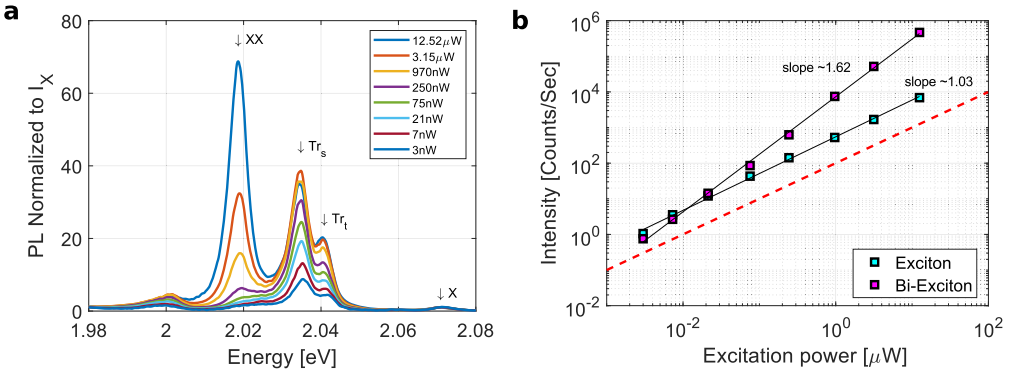

Figure 4. Highly efficient biexciton emission. (a) Normalized PL spectra for different cw excitation power ranging from μW to nW, showing that the XX emission peak can be observed at excitations powers down to few nW. (b) Linear fits of the exciton and biexciton PL emission showing the superlinear behavior of the biexcitons peak. The dashed red line correspond to slope = 1.

Equation 3 implies a linear relationship between $A_{max}\gamma_T/\xi_1$ and $1/\gamma_T$, provided that $\gamma_d/\gamma_T \ll 1$. Indeed, the universal law is confirmed by the experimental data from different samples and locations presented in Figure 2c. The different samples follow their own straight line, which encodes their different quality, but the generic behavior is the same for all. In addition, $\gamma_{r,0}$ of the different samples can be extracted from the (extrapolated) crossing point $1/\gamma_T = 0$. In principle, this universal law should hold for any 2D excitonic system where $\gamma_d \ll \gamma_T$.

Another important outcome of this analysis is the ability to compare different excitonic properties via their absorption response. Figure 2d shows the extracted temperature-dependent γ_{nr} and γ_d (see SI) and their phenomenological fit.[46,53] These correlate directly with their absorption behavior, indicating that higher dephasing leads to lower absorption.

In the same manner, we have designed the VHC for maximal interaction strength, it can be designed to any intermediate value, and even to completely turn off the interaction between the light and the TMD. To demonstrate this, we fabricated on the same device two different cavities, one for which the interaction is optimized (denoted as "on") and one for which the interaction is minimized (denoted as "off"). This is done by adding another hBN flake below a part of the heterostructure. The spatial distribution of the absorption for this device at T = 300 K is presented in Figure 3a (see SI for exemplary spectral curves) and its extracted exciton line width distribution in Figure 3b. The spatial correlation between the absorption and line width can be directly observed in the "on" areas of the two figures, that is, lower line width correlates to higher absorption, which is indeed the case for T = 300 K (see Figure 1d). The source of the spatial distribution comes from the inhomogeneity of the sample, a well-known issue in TMDs.[47] Furthermore, the extracted γ_r from the two cavities yields 2.2 meV and 70 μeV in the "on" and "off" regions, respectively. This is in agreement with the Purcell effect line width modulation obtained by refs 59−62.

The ability to achieve near-unity excitonic absorption implies that a large photoexcited excitonic density can be obtained, while maintaining low excitation power. It was already shown that TMDs are highly affected by the excitation power, resulting in either heating effects that changes the excitonic properties temporarily,[63] or permanent effects that completely alter the material's response, such as optical doping and environmental surface interactions.[5,64] Yet, this challenging and desirable high exciton density plays a major role in several physical phenomena, such as Bosonic condensation, phase transitions,[65] and biexcitons emission,[5] for example. The formation of biexcitons is directly related to high excitonic density and thus also to the possible appearance of the biexciton peak in the PL spectrum.[5] The predicted intensity relation between the exciton and biexciton emission is a power law, $I_{XX} = I_X^{\alpha}$, with α ranging between 1.2−1.9 due to lack of thermal equilibrium.[5] Thus, the latter can be used to probe the efficiency of exciton photogeneration in the VHC.

Figure 4a shows the PL spectra, normalized to the exciton emission intensity (I_X), obtained from the VHC for different cw excitation powers. Several peaks can be observed and are marked as X, exciton at E = 2.071 eV; Tr_t/Tr_s, singlet/triplet trions[50] at 2.034 eV/2.04 eV, respectively; and XX, biexciton at E = 2.018 eV. Remarkably, the XX emission peak can be observed at excitations powers down to few nW. This excitation power is 2−3 orders of magnitude smaller than the lowest previously reported for biexcitons.[44] Actually, for excitation powers above 30 μW, the XX emission intensity is so high that it saturates our detector. Figure 4b shows the power law analysis of the I_{XX} and I_X peaks, and the obtained α = 1.62 for I_{XX} confirms the identity of the biexciton. From the maximal used power of 400 μW, we can calculate an excitonic density of ~2.5×10^{11} cm^{-2}. This exciton density is 2 orders of magnitude larger than what was achieved in previous works using cw excitation, and is similar to densities obtained using ultrafast laser pulses.[29] While it is possible that at high cw excitation powers heating effects may kick in, using pulsed excitation (as in ref 29 for example) with our VHC, one can obtain an excitonic density of ~5×10^{13} cm^{-2} with little heating, as compared to ~6.4×10^{12} cm^{-2}.

In conclusion, the new type of optical cavity presented here, which is based solely on VdW heterostructures, is designed for ultrastrong light-exciton interaction, and unveils a universal absorption law for excitons in 2D systems. This enhanced light-exciton interaction can act as a platform for probing quantum nonlinear dynamics of excitons[46,48] and their state of matter,[65] and paves the way to efficient optoelectronic devices, such as detectors, modulators, and optically pumped light emitting devices, based on monolayer semiconductors. Specifically, this high absorption is important for TMD-based photodetectors, as the internal photodetection efficiency of TMDs has been demonstrated to be high,[66] but the external efficiency has always been limited by the low absorption efficiency.

https://dx.doi.org/10.1021/acs.nanolett.0c00492
Nano Lett. 2020, 20, 3545−3552

■ ASSOCIATED CONTENT

Supporting Information

The Supporting Information is available free of charge at https://pubs.acs.org/doi/10.1021/acs.nanolett.0c00492.

Theoretical modeling, fitting procedure, identification of excitonic complexes, structure optimization, and experimental and fabrication methods (PDF)

■ AUTHOR INFORMATION

Corresponding Authors

Itai Epstein − *ICFO-Institut de Ciencies Fotoniques, The Barcelona Institute of Science and Technology, 08860 Castelldefels, Barcelona, Spain;* orcid.org/0000-0002-6174-4025; Email: itai.epstein@icfo.eu

Frank H. L. Koppens − *ICFO-Institut de Ciencies Fotoniques, The Barcelona Institute of Science and Technology, 08860 Castelldefels, Barcelona, Spain; ICREA—Institució Catalana de Recerca i Estudis Avançats, 08010 Barcelona, Spain;* orcid.org/0000-0001-9764-6120; Email: frank.koppens@icfo.eu

Authors

Bernat Terrés − *ICFO-Institut de Ciencies Fotoniques, The Barcelona Institute of Science and Technology, 08860 Castelldefels, Barcelona, Spain*

André J. Chaves − *Grupo de Materiais Semicondutores e Nanotecnologia and Departamento de Fisica, Instituto Tecnológico de Aeronáutica, 12228-900 São José dos Campos,, Brazil*

Varun-Varma Pusapati − *ICFO-Institut de Ciencies Fotoniques, The Barcelona Institute of Science and Technology, 08860 Castelldefels, Barcelona, Spain*

Daniel A. Rhodes − *Department of Mechanical Engineering, Columbia University, New York, New York 10027, United States*

Bettina Frank − *Fourth Physics Institute and Research Center SCoPE, University of Stuttgart, 70569 Stuttgart, Germany*

Valentin Zimmermann − *Fourth Physics Institute and Research Center SCoPE, University of Stuttgart, 70569 Stuttgart, Germany*

Ying Qin − *School for Engineering of Matter Transport and Energy, Arizona State University, Tempe, Arizona 85287, United States*

Kenji Watanabe − *National Institute for Materials Science, Tsukuba 305-0044, Japan;* orcid.org/0000-0003-3701-8119

Takashi Taniguchi − *National Institute for Materials Science, Tsukuba 305-0044, Japan;* orcid.org/0000-0002-1467-3105

Harald Giessen − *Fourth Physics Institute and Research Center SCoPE, University of Stuttgart, 70569 Stuttgart, Germany*

Sefaattin Tongay − *School for Engineering of Matter Transport and Energy, Arizona State University, Tempe, Arizona 85287, United States;* orcid.org/0000-0001-8294-984X

James C. Hone − *Department of Mechanical Engineering, Columbia University, New York, New York 10027, United States*

Nuno M. R. Peres − *Centro de Física and Departamento de Física and QuantaLab, Universidade do Minho, P-4710-057 Braga, Portugal; International Iberian Nanotechnology Laboratory (INL), 4715-330 Braga, Portugal*

Complete contact information is available at: https://pubs.acs.org/10.1021/acs.nanolett.0c00492

Author Contributions

[▽]I.E. and B.T. contributed equally.

Notes

The authors declare no competing financial interest.

■ ACKNOWLEDGMENTS

The authors thank Mr. David Alcaraz Iranzo, Dr. Fabien Vialla, and Dr. Antoine Reserbat-Plantey for fruitful discussions. F.H.L.K. acknowledges financial support from the Spanish Ministry of Economy and Competitiveness through the "Severo Ochoa" Programme for Centres of Excellence in R and D (SEV-2015-0522), support by Fundacio Cellex Barcelona, Generalitat de Catalunya through the CERCA program, and the Mineco grants Ramon y Cajal (RYC-2012-12281, Plan Nacional (FIS2013-47161-P and FIS2014-59639-JIN), and the Agency for Management of University and Research Grants (AGAUR) 2017 SGR 1656. Furthermore, the research leading to these results has received funding from the European Union Seventh Framework Programme under grant agreement numbers 785219 and 881603 Graphene Flagship. This work was supported by the ERC TOPONANOP under grant agreement number 726001 and the MINECO Plan Nacional Grant 2D-NANOTOP under reference number FIS2016-81044-P. S.T. acknowledges support from NSF DMR-1552220 and DMR-1838443. N.M.R.P acknowledges financing from European Commission through the project "Graphene-Driven Revolutions in ICT and Beyond" (ref. no. 785219) and from FEDER and the Portuguese Foundation for Science and Technology (FCT) through project POCI-01-0145-FEDER-028114. H.G. and B.F. acknowledge support from ERC advanced grant COMPLEXPLAS. J.H. and D.R. acknowledge the funding support by the NSF MRSEC program through Columbia in the Center for Precision Assembly of Superstratic and Superatomic Solids (DMR-1420634).

■ REFERENCES

(1) Xu, X.; Yao, W.; Xiao, D.; Heinz, T. F. Spin and pseudospins in layered transition metal dichalcogenides. *Nat. Phys.* **2014**, *10*, 343−350.

(2) Mueller, T.; Malic, E. Exciton physics and device application of two-dimensional transition metal dichalcogenide semiconductors. *npj 2D Materials and Applications* **2018**, *2*, 29.

(3) Mak, K. F.; He, K.; Lee, C.; Lee, G. H.; Hone, J.; Heinz, T. F.; Shan, J. Tightly bound trions in monolayer MoS_2. *Nat. Mater.* **2013**, *12*, 207−211.

(4) Ross, J. S.; Wu, S.; Yu, H.; Ghimire, N. J.; Jones, A. M.; Aivazian, G.; Yan, J.; Mandrus, D. G.; Xiao, D.; Yao, W.; Xu, X. Electrical control of neutral and charged excitons in a monolayer semiconductor. *Nat. Commun.* **2013**, *4*, 1474.

(5) You, Y.; Zhang, X.-X.; Berkelbach, T. C.; Hybertsen, M. S.; Reichman, D. R.; Heinz, T. F. Observation of biexcitons in monolayer WSe_2. *Nat. Phys.* **2015**, *11*, 477−481.

(6) Plechinger, G.; Nagler, P.; Kraus, J.; Paradiso, N.; Strunk, C.; Schüller, C.; Korn, T. Identification of excitons, trions and biexcitons in single-layer WS_2. *Phys. Status Solidi RRL* **2015**, *9*, 457−461.

(7) Xiao, D.; Liu, G.-B.; Feng, W.; Xu, X.; Yao, W. Coupled Spin and Valley Physics in Monolayers of MoS_2 and Other Group-VI Dichalcogenides. *Phys. Rev. Lett.* **2012**, *108*, 196802.

(8) Zeng, H.; Dai, J.; Yao, W.; Xiao, D.; Cui, X. Valley polarization in MoS_2 monolayers by optical pumping. *Nat. Nanotechnol.* **2012**, *7*, 490−493.

(9) Mak, K. F.; He, K.; Shan, J.; Heinz, T. F. Control of valley polarization in monolayer MoS_2 by optical helicity. *Nat. Nanotechnol.* **2012**, *7*, 494−498.
(10) Cao, T.; Wang, G.; Han, W.; Ye, H.; Zhu, C.; Shi, J.; Niu, Q.; Tan, P.; Wang, E.; Liu, B.; Feng, J. Valley-selective circular dichroism of monolayer molybdenum disulphide. *Nat. Commun.* **2012**, *3*, 887.
(11) Tonndorf, P.; Schmidt, R.; Schneider, R.; Kern, J.; Buscema, M.; Steele, G. A.; Castellanos-Gomez, A.; van der Zant, H. S. J.; Michaelis de Vasconcellos, S.; Bratschitsch, R. Single-photon emission from localized excitons in an atomically thin semiconductor. *Optica* **2015**, *2*, 347.
(12) Chakraborty, C.; Kinnischtzke, L.; Goodfellow, K. M.; Beams, R.; Vamivakas, A. N. Voltage-controlled quantum light from an atomically thin semiconductor. *Nat. Nanotechnol.* **2015**, *10*, 507−511.
(13) Koperski, M.; Nogajewski, K.; Arora, A.; Cherkez, V.; Mallet, P.; Veuillen, J.-Y.; Marcus, J.; Kossacki, P.; Potemski, M. Single photon emitters in exfoliated WSe_2 structures. *Nat. Nanotechnol.* **2015**, *10*, 503−506.
(14) He, Y.-M.; Clark, G.; Schaibley, J. R.; He, Y.; Chen, M.-C.; Wei, Y.-J.; Ding, X.; Zhang, Q.; Yao, W.; Xu, X.; Lu, C.-Y.; Pan, J.-W. Single quantum emitters in monolayer semiconductors. *Nat. Nanotechnol.* **2015**, *10*, 497−502.
(15) Srivastava, A.; Sidler, M.; Allain, A. V.; Lembke, D. S.; Kis, A.; Imamoğlu, A. Optically active quantum dots in monolayer WSe_2. *Nat. Nanotechnol.* **2015**, *10*, 491−496.
(16) Radisavljevic, B.; Radenovic, A.; Brivio, J.; Giacometti, V.; Kis, A. Single-layer MoS_2 transistors. *Nat. Nanotechnol.* **2011**, *6*, 147−150.
(17) Yin, Z.; Li, H.; Li, H.; Jiang, L.; Shi, Y.; Sun, Y.; Lu, G.; Zhang, Q.; Chen, X.; Zhang, H. Single-Layer MoS_2 Phototransistors. *ACS Nano* **2012**, *6*, 74−80.
(18) Lopez-Sanchez, O.; Lembke, D.; Kayci, M.; Radenovic, A.; Kis, A. Ultrasensitive photodetectors based on monolayer MoS_2. *Nat. Nanotechnol.* **2013**, *8*, 497−501.
(19) Baugher, B. W. H.; Churchill, H. O. H.; Yang, Y.; Jarillo-Herrero, P. Optoelectronic devices based on electrically tunable p−n diodes in a monolayer dichalcogenide. *Nat. Nanotechnol.* **2014**, *9*, 262−267.
(20) Ross, J. S.; Klement, P.; Jones, A. M.; Ghimire, N. J.; Yan, J.; Mandrus, D. G.; Taniguchi, T.; Watanabe, K.; Kitamura, K.; Yao, W.; Cobden, D. H.; Xu, X. Electrically tunable excitonic light-emitting diodes based on monolayer WSe_2 p−n junctions. *Nat. Nanotechnol.* **2014**, *9*, 268−272.
(21) Mak, K. F.; Shan, J. Photonics and optoelectronics of 2D semiconductor transition metal dichalcogenides. *Nat. Photonics* **2016**, *10*, 216−226.
(22) Wang, G.; Chernikov, A.; Glazov, M. M.; Heinz, T. F.; Marie, X.; Amand, T.; Urbaszek, B. Colloquium: Excitons in atomically thin transition metal dichalcogenides. *Rev. Mod. Phys.* **2018**, *90*, 021001.
(23) Wurstbauer, U.; Miller, B.; Parzinger, E.; Holleitner, A. W. Light−matter interaction in transition metal dichalcogenides and their heterostructures. *J. Phys. D: Appl. Phys.* **2017**, *50*, 173001.
(24) Britnell, L.; Ribeiro, R. M.; Eckmann, A.; Jalil, R.; Belle, B. D.; Mishchenko, A.; Kim, Y.-J.; Gorbachev, R. V.; Georgiou, T.; Morozov, S. V.; Grigorenko, A. N.; Geim, A. K.; Casiraghi, C.; Neto, A. H. C.; Novoselov, K. S. Strong Light-Matter Interactions in Heterostructures of Atomically Thin Films. *Science* **2013**, *340*, 1311−1314.
(25) Liu, X.; Galfsky, T.; Sun, Z.; Xia, F.; Lin, E.-c.; Lee, Y.-H.; Kéna-Cohen, S.; Menon, V. M. Strong light−matter coupling in two-dimensional atomic crystals. *Nat. Photonics* **2015**, *9*, 30−34.
(26) Schneider, C.; Glazov, M. M.; Korn, T.; Höfling, S.; Urbaszek, B. Two-dimensional semiconductors in the regime of strong light-matter coupling. *Nat. Commun.* **2018**, *9*, 2695.
(27) Chernikov, A.; Berkelbach, T. C.; Hill, H. M.; Rigosi, A.; Li, Y.; Aslan, O. B.; Reichman, D. R.; Hybertsen, M. S.; Heinz, T. F. Exciton Binding Energy and Nonhydrogenic Rydberg Series in Monolayer WS_2. *Phys. Rev. Lett.* **2014**, *113*, 076802.
(28) Ugeda, M. M.; Bradley, A. J.; Shi, S.-F.; da Jornada, F. H.; Zhang, Y.; Qiu, D. Y.; Ruan, W.; Mo, S.-K.; Hussain, Z.; Shen, Z.-X.; Wang, F.; Louie, S. G.; Crommie, M. F. Giant bandgap renormalization and excitonic effects in a monolayer transition metal dichalcogenide semiconductor. *Nat. Mater.* **2014**, *13*, 1091−1095.
(29) Poellmann, C.; Steinleitner, P.; Leierseder, U.; Nagler, P.; Plechinger, G.; Porer, M.; Bratschitsch, R.; Schüller, C.; Korn, T.; Huber, R. Resonant internal quantum transitions and femtosecond radiative decay of excitons in monolayer WSe_2. *Nat. Mater.* **2015**, *14*, 889−893.
(30) Robert, C.; Lagarde, D.; Cadiz, F.; Wang, G.; Lassagne, B.; Amand, T.; Balocchi, A.; Renucci, P.; Tongay, S.; Urbaszek, B.; Marie, X. Exciton radiative lifetime in transition metal dichalcogenide monolayers. *Phys. Rev. B: Condens. Matter Mater. Phys.* **2016**, *93*, 205423.
(31) Okada, M.; Miyauchi, Y.; Matsuda, K.; Taniguchi, T.; Watanabe, K.; Shinohara, H.; Kitaura, R. Observation of biexcitonic emission at extremely low power density in tungsten disulfide atomic layers grown on hexagonal boron nitride. *Sci. Rep.* **2017**, *7*, 322.
(32) Li, Y.; Chernikov, A.; Zhang, X.; Rigosi, A.; Hill, H. M.; van der Zande, A. M.; Chenet, D. A.; Shih, E.-M.; Hone, J.; Heinz, T. F. Measurement of the optical dielectric function of monolayer transition-metal dichalcogenides: MoS_2, $MoSe_2$, WS_2, and WSe_2. *Phys. Rev. B: Condens. Matter Mater. Phys.* **2014**, *90*, 205422.
(33) Bahauddin, S. M.; Robatjazi, H.; Thomann, I. Broadband Absorption Engineering to Enhance Light Absorption in Monolayer MoS_2. *ACS Photonics* **2016**, *3*, 853−862.
(34) Liu, J.-T.; Wang, T.-B.; Li, X.-J.; Liu, N.-H. Enhanced absorption of monolayer MoS_2 with resonant back reflector. *J. Appl. Phys.* **2014**, *115*, 193511.
(35) Wang, Q.; Guo, J.; Ding, Z.; Qi, D.; Jiang, J.; Wang, Z.; Chen, W.; Xiang, Y.; Zhang, W.; Wee, A. T. S. Fabry−Perot Cavity-Enhanced Optical Absorption in Ultrasensitive Tunable Photodiodes Based on Hybrid 2D Materials. *Nano Lett.* **2017**, *17*, 7593−7598.
(36) Mak, K. F.; He, K.; Lee, C.; Lee, G. H.; Hone, J.; Heinz, T. F.; Shan, J. Tightly bound trions in monolayer MoS_2. *Nat. Mater.* **2013**, *12*, 207−211.
(37) Zhang, C.; Wang, H.; Chan, W.; Manolatou, C.; Rana, F. Absorption of light by excitons and trions in monolayers of metal dichalcogenide MoS_2: Experiments and theory. *Phys. Rev. B: Condens. Matter Mater. Phys.* **2014**, *89*, 205436.
(38) Jariwala, D.; Davoyan, A. R.; Tagliabue, G.; Sherrott, M. C.; Wong, J.; Atwater, H. A. Near-Unity Absorption in van der Waals Semiconductors for Ultrathin Optoelectronics. *Nano Lett.* **2016**, *16*, 5482−5487.
(39) Li, H.; Qin, M.; Wang, L.; Zhai, X.; Ren, R.; Hu, J. Total absorption of light in monolayer transition-metal dichalcogenides by critical coupling. *Opt. Express* **2017**, *25*, 31612.
(40) Liu, D.; Chen, H. Atomically thin planar metasurfaces. *J. Photonics Energy* **2019**, *9*, 1.
(41) Li, Z.; Xiao, Y.; Gong, Y.; Wang, Z.; Kang, Y.; Zu, S.; Ajayan, P. M.; Nordlander, P.; Fang, Z. Active Light Control of the MoS_2 Monolayer Exciton Binding Energy. *ACS Nano* **2015**, *9*, 10158−10164.
(42) Cadiz, F.; et al. Excitonic Linewidth Approaching the Homogeneous Limit in MoS2 -Based van der Waals Heterostructures. *Phys. Rev. X* **2017**, *7*, 021026.
(43) Ajayi, O. A.; Ardelean, J. V.; Shepard, G. D.; Wang, J.; Antony, A.; Taniguchi, T.; Watanabe, K.; Heinz, T. F.; Strauf, S.; Zhu, X.-Y.; Hone, J. C. Approaching the intrinsic photoluminescence linewidth in transition metal dichalcogenide monolayers. *2D Mater.* **2017**, *4*, 031011.
(44) Ye, Z.; Waldecker, L.; Ma, E. Y.; Rhodes, D.; Antony, A.; Kim, B.; Zhang, X.-X.; Deng, M.; Jiang, Y.; Lu, Z.; Smirnov, D.; Watanabe, K.; Taniguchi, T.; Hone, J.; Heinz, T. F. Efficient generation of neutral and charged biexcitons in encapsulated WSe_2 monolayers. *Nat. Commun.* **2018**, *9*, 3718.
(45) Barbone, M.; et al. Charge-tuneable biexciton complexes in monolayer WSe_2. *Nat. Commun.* **2018**, *9*, 3721.
(46) Scuri, G.; Zhou, Y.; High, A. A.; Wild, D. S.; Shu, C.; De Greve, K.; Jauregui, L. A.; Taniguchi, T.; Watanabe, K.; Kim, P.; Lukin, M.

https://dx.doi.org/10.1021/acs.nanolett.0c00492
Nano Lett. 2020, 20, 3545−3552

D.; Park, H. Large Excitonic Reflectivity of Monolayer $MoSe_2$ Encapsulated in Hexagonal Boron Nitride. *Phys. Rev. Lett.* **2018**, *120*, 037402.
(47) Back, P.; Zeytinoglu, S.; Ijaz, A.; Kroner, M.; Imamoğlu, A. Realization of an Electrically Tunable Narrow-Bandwidth Atomically Thin Mirror Using Monolayer $MoSe_2$. *Phys. Rev. Lett.* **2018**, *120*, 037401.
(48) Zeytinoğlu, S.; Roth, C.; Huber, S.; İmamoğlu, A. Atomically thin semiconductors as nonlinear mirrors. *Phys. Rev. A: At., Mol., Opt. Phys.* **2017**, *96*, 031801.
(49) Podbiel, D.; Kahl, P.; Frank, B.; Davis, T. J.; Giessen, H.; Hoegen, M. H.-v.; Meyer zu Heringdorf, F. J. Spatiotemporal Analysis of an Efficient Fresnel Grating Coupler for Focusing Surface Plasmon Polaritons. *ACS Photonics* **2019**, *6*, 600−604.
(50) Plechinger, G.; Nagler, P.; Arora, A.; Schmidt, R.; Chernikov, A.; del Águila, A. G.; Christianen, P. C.; Bratschitsch, R.; Schüller, C.; Korn, T. Trion fine structure and coupled spin−valley dynamics in monolayer tungsten disulfide. *Nat. Commun.* **2016**, *7*, 12715.
(51) Paur, M.; Molina-Mendoza, A. J.; Bratschitsch, R.; Watanabe, K.; Taniguchi, T.; Mueller, T. Electroluminescence from multi-particle exciton complexes in transition metal dichalcogenide semiconductors. *Nat. Commun.* **2019**, *10*, 1709.
(52) Rudin, S.; Reinecke, T. L.; Segall, B. Temperature-dependent exciton linewidths in semiconductors. *Phys. Rev. B: Condens. Matter Mater. Phys.* **1990**, *42*, 11218−11231.
(53) Selig, M.; Berghäuser, G.; Raja, A.; Nagler, P.; Schüller, C.; Heinz, T. F.; Korn, T.; Chernikov, A.; Malic, E.; Knorr, A. Excitonic linewidth and coherence lifetime in monolayer transition metal dichalcogenides. *Nat. Commun.* **2016**, *7*, 13279.
(54) Combescot, M.; Betbeder-Matibet, O.; Leuenberger, M. N. Analytical approach to semiconductor Bloch equations. *EPL (Europhysics Letters)* **2009**, *88*, 57007.
(55) Chaves, A. J.; Ribeiro, R. M.; Frederico, T.; Peres, N. M. R. Excitonic effects in the optical properties of 2D materials:an equation of motion approach. *2D Mater.* **2017**, *4*, 025086.
(56) Efimkin, D. K.; MacDonald, A. H. Many-body theory of trion absorption features in two-dimensional semiconductors. *Phys. Rev. B: Condens. Matter Mater. Phys.* **2017**, *95*, 035417.
(57) Chang, Y. W.; Reichman, D. R. Many-body theory of optical absorption in doped two-dimensional semiconductors. *Phys. Rev. B: Condens. Matter Mater. Phys.* **2019**, *99*, 125421.
(58) Thongrattanasiri, S.; Koppens, F. H. L.; García de Abajo, F. J. Complete Optical Absorption in Periodically Patterned Graphene. *Phys. Rev. Lett.* **2012**, *108*, 047401.
(59) Fang, H.; Han, B.; Robert, C.; Semina, M.; Lagarde, D.; Courtade, E.; Taniguchi, T.; Watanabe, K.; Amand, T.; Urbaszek, B.; Glazov, M.; Marie, X. Control of the Exciton Radiative Lifetime in van der Waals Heterostructures. *Phys. Rev. Lett.* **2019**, *123*, 067401.
(60) Horng, J.; Chou, Y.-H.; Chang, T.-C.; Hsu, C.-Y.; Lu, T.-C.; Deng, H. Engineering radiative coupling of excitons in 2D semiconductors. *Optica* **2019**, *6*, 1443.
(61) Zhou, Y.; Scuri, G.; Sung, J.; Gelly, R. J.; Wild, D. S.; De Greve, K.; Joe, A. Y.; Taniguchi, T.; Watanabe, K.; Kim, P.; Lukin, M. D.; Park, H. Controlling Excitons in an Atomically Thin Membrane with a Mirror. *Phys. Rev. Lett.* **2020**, *124*, 027401.
(62) Rogers, C.; Gray, D.; Bogdanowicz, N.; Taniguchi, T.; Watanabe, K.; Mabuchi, H. Coherent feedback control of two-dimensional excitons. *Physical Review Research* **2020**, *2*, 012029.
(63) Currie, M.; Hanbicki, A. T.; Kioseoglou, G.; Jonker, B. T. Optical control of charged exciton states in tungsten disulfide. *Appl. Phys. Lett.* **2015**, *106*, 201907.
(64) Cadiz, F.; et al. Ultra-low power threshold for laser induced changes in optical properties of 2D molybdenum dichalcogenides. *2D Mater.* **2016**, *3*, 045008.
(65) Arp, T. B.; Pleskot, D.; Aji, V.; Gabor, N. M. Electron−hole liquid in a van der Waals heterostructure photocell at room temperature. *Nat. Photonics* **2019**, *13*, 245−250.
(66) Massicotte, M.; Schmidt, P.; Vialla, F.; Schädler, K. G.; Reserbat-Plantey, A.; Watanabe, K.; Taniguchi, T.; Tielrooij, K. J.; Koppens, F. H. Picosecond photoresponse in van der Waals heterostructures. *Nat. Nanotechnol.* **2016**, *11*, 42−46.

https://dx.doi.org/10.1021/acs.nanolett.0c00492
Nano Lett. 2020, 20, 3545−3552